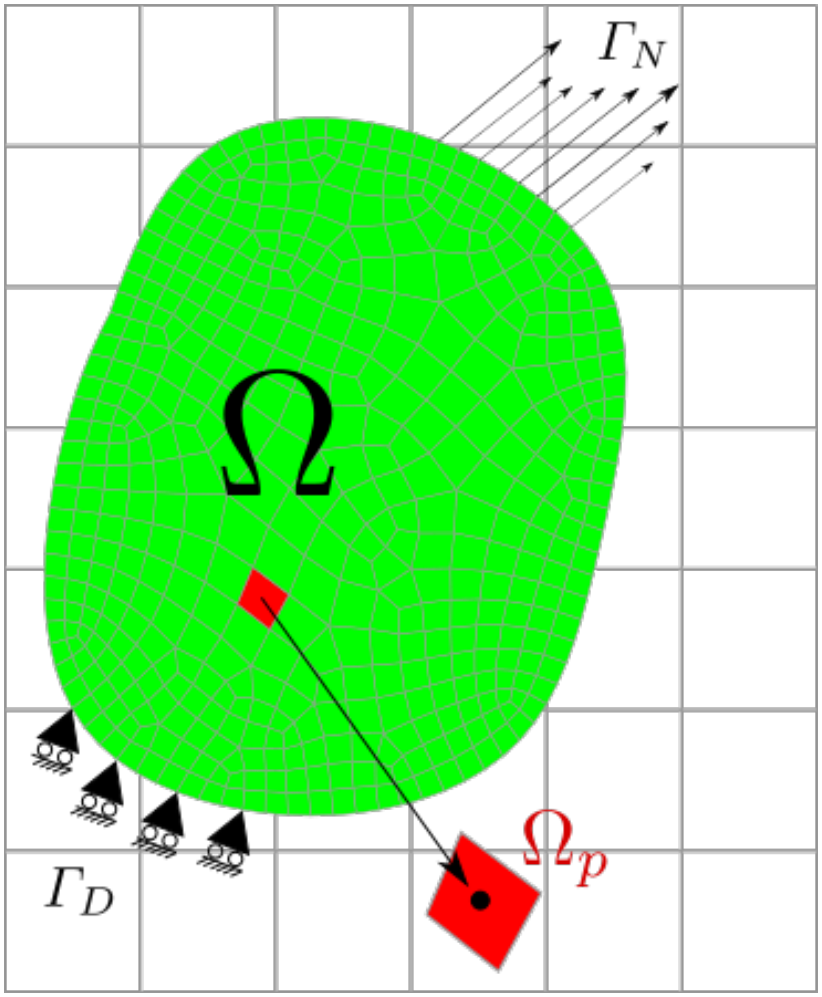

Figure 1: Discretization used in the material point method.

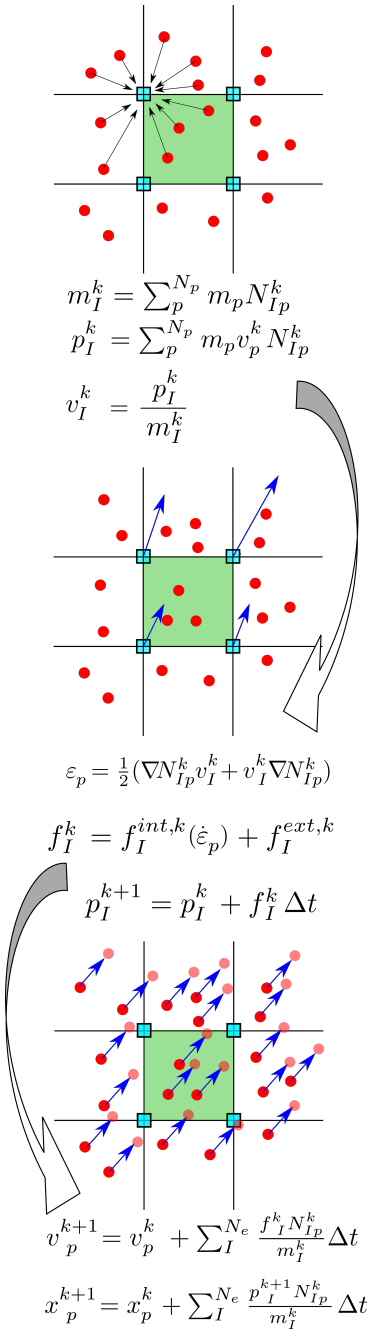

Figure 2: Classic material point method algorithm.

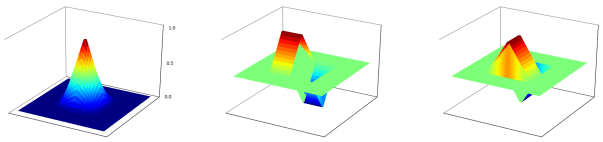

(a) Piecewise linear (Q4).

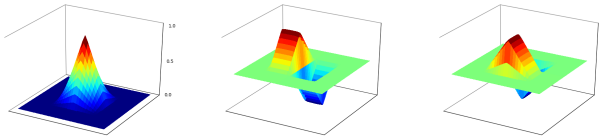

(b) Local *max-ent* $\gamma = 17$.

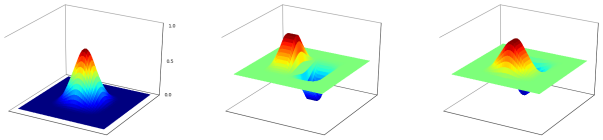

(c) Uniform GIMP (uGIMP).

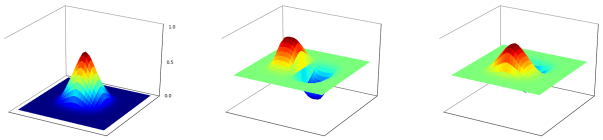

(d) Local *max-ent* $\gamma = 10$.

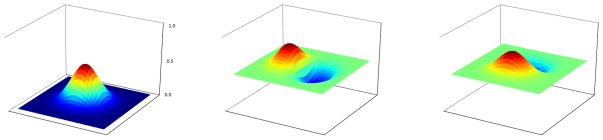

(e) Local *max-ent* $\gamma = 7$.

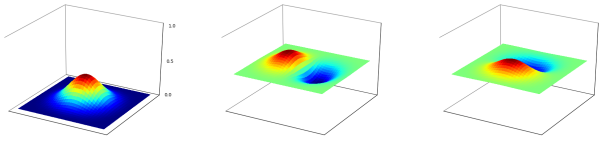

(f) Local *max-ent* $\gamma = 5$.

Figure 3: Comparison of the local *max-ent* shape function for different values of $\gamma = \beta h^2$, the piecewise linear shape function and the uniform GIMP shape function. The picture shows the nodal value of each shape function and its derivatives evaluated in a material point located in the center of the domain.

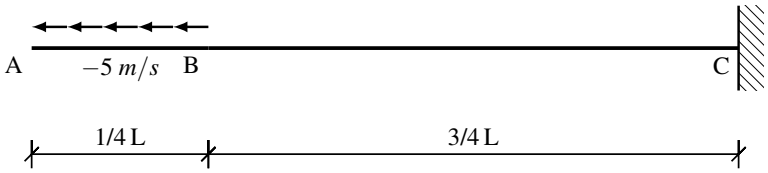

Figure 4: Geometrical description of the Dyka [**?**] bar.

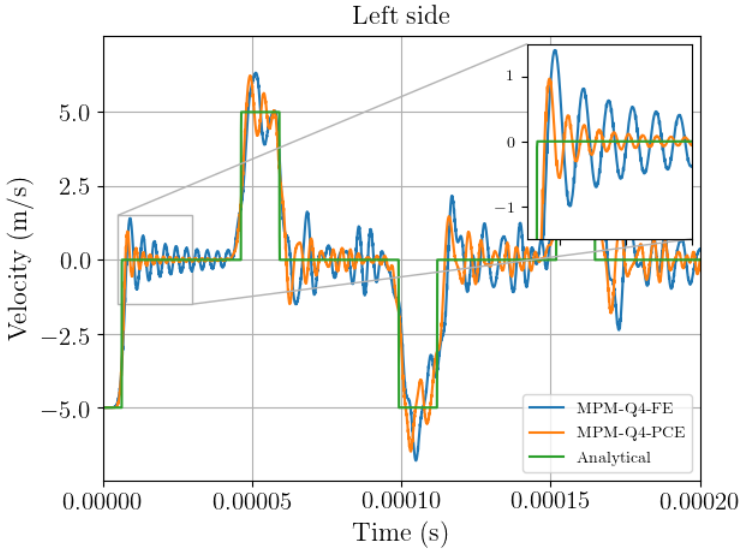

Figure 5: Velocity evolution in the bar left side. This picture shows a comparison between both time integration algorithms, the Forward-Euler (FE) and the Predictor-Corrector explicit (PCE).

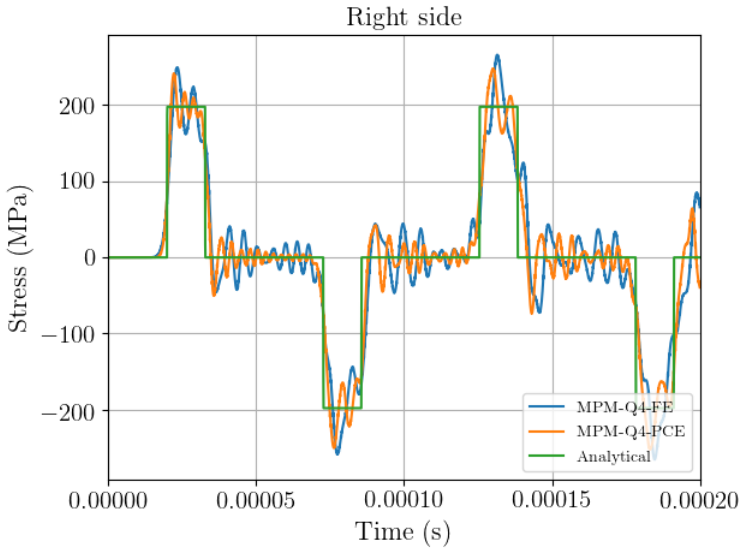

Figure 6: Stress evolution in the bar left side. This picture shows a comparison between both time integration algorithms, the Forward-Euler (FE) and the Predictor-Corrector explicit (PCE).

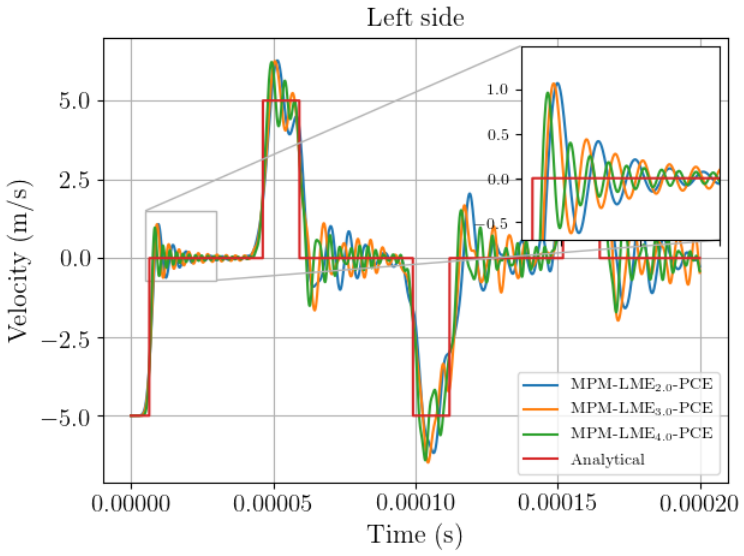

Figure 7: Velocity evolution in the bar left side. This picture shows how variation of affect in a simulation with no grid grossing.

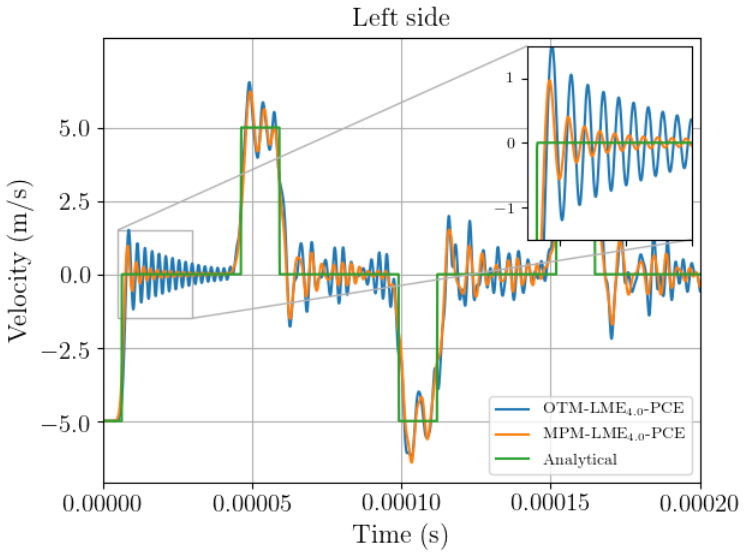

Figure 8: Velocity evolution in the bar left side. This picture shows a comparison between the optimal transportation mesh-free (OTM) method and the material point method (MPM) using the same time integration scheme and and spacial discretization.

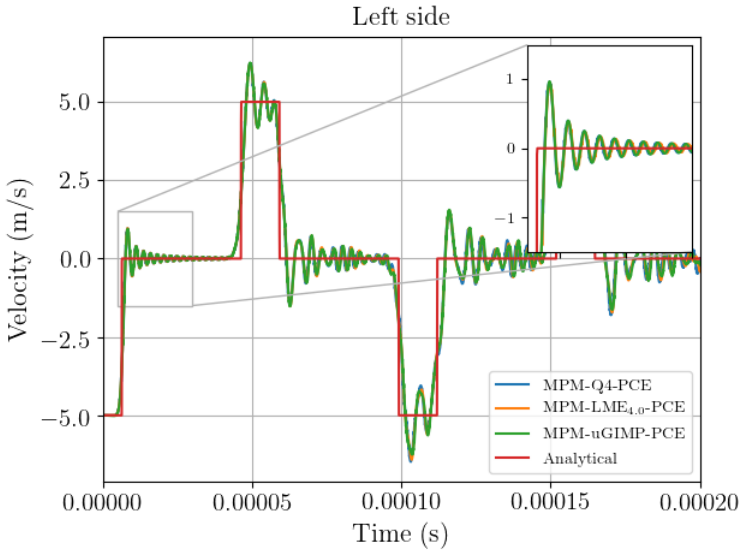

Figure 9: Velocity evolution in the bar left side. This picture shows a comparison between the three different interpolation techniques using the explicit predictor corrector to perform the simulations.

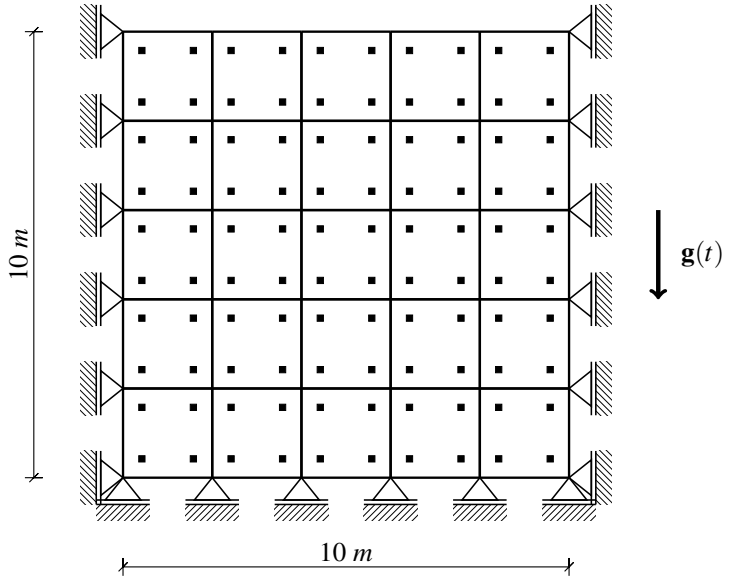

Figure 10: Initial setting of material points and grid nodes in the soil block. The soil is fixed horizontally along the vertical walls and vertically along the bottom. The units of the axis are meters.

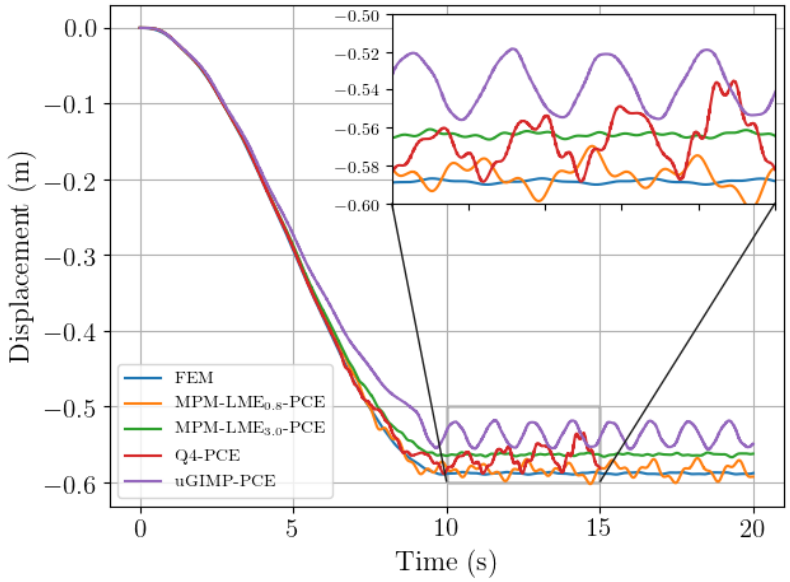

Figure 11: Comparative of the vertical displacement evolution in a point located in the free surface employing different interpolation schemes and numerical techniques.

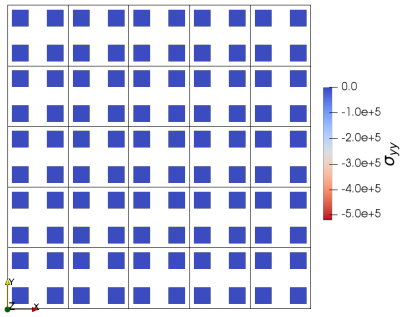

(a) t = 0 seconds.

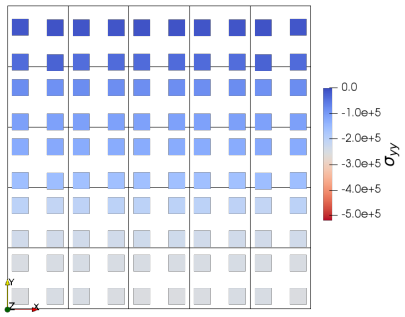

(b) t = 5 seconds.

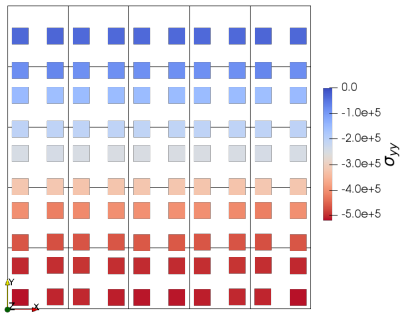

(c) t = 20 seconds

Figure 12: Vertical normal stress and position of material points during the loading process for a soft soil ($E = 5\ MPa$, $\rho_0 = 6 \cdot 10^3\ kg/m^3$). Numerical parameters considered for the simulation are : Local *max-ent* shape function $\gamma = 3$ and explicit PC scheme with CFL 0.1.

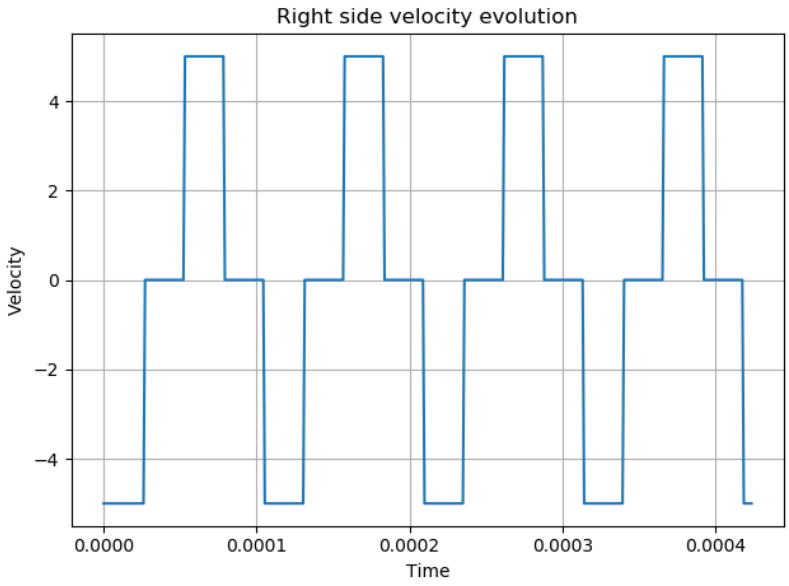

Figure 13: Analytical solution for the velocity in the right side of the Dyka bar.

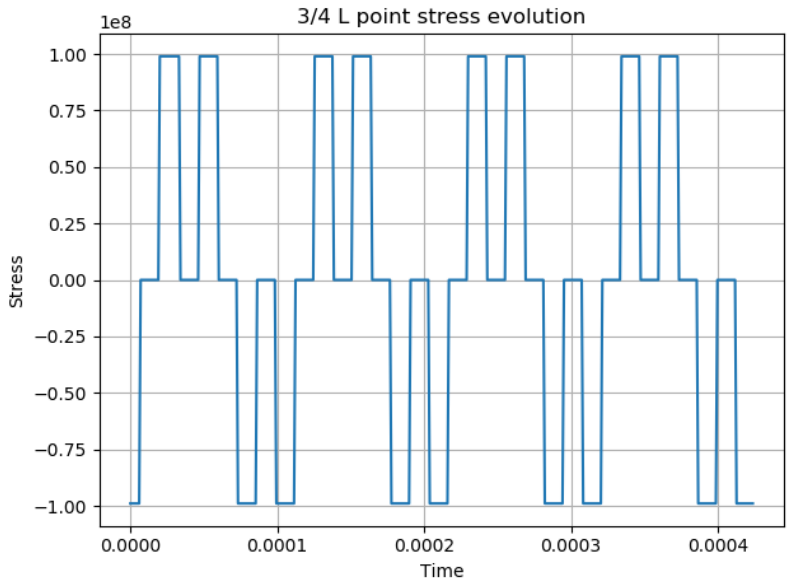

Figure 14: Analytical solution for the stress in the last quarter of the Dyka bar.